# Sputtering yields exceeding 1000 by 80 keV Xe irradiation of Au nanorods

A. Ilinov[1], A. Kuronen[1], K. Nordlund[1], G. Greaves[2], J. A. Hinks[2], P. Busby[3], N. J. Mellors[3], and S. E. Donnelly[2]

[1]*Department of Physics, University of Helsinki, P.O. Box 43, Helsinki FI–00014, Finland*

[2]*School of Computing and Engineering, University of Huddersfield, Huddersfield HD1 3DH, UK*

[3]*School of Computing, Science and Engineering, University of Salford Manchester M5 4WT, UK*

Using experiments and computer simulations, we find that 80 keV Xe ion irradiation of Au nanorods can produce sputtering yields exceeding 1000, which to our knowledge are the highest yields reported for sputtering by single ions in the nuclear collision regime. This value is enhanced by more than an order of magnitude compared to the same irradiation of flat Au surfaces. Using MD simulations, we show that the very high yield can be understood as a combination of enhanced yields due to low incoming angles at the sides of the nanowire, as well as the high surface-to-volume ratio causing enhanced explosive sputtering from heat spikes. We also find, both in experiments and simulations, that channeling has a strong effect on the sputtering yield: if the incoming beam happens to be aligned with a crystal axis of the nanorod, the yield can decrease to about 100.

PACS numbers: 61.05.J-, 61.46.Km, 61.80.Jh, 61.80.Az

## 1. Introduction

Single heavy ion impacts on flat surfaces of dense metals cause changes in surface topography that involve the displacement of tens of thousands of atoms and can give rise to the formation of features such as craters and mounds with dimensions of the order of 10 nm [1–4]. This can be understood in terms of localized processes occurring during the thermal spike part of the energy dissipation process [5] and can lead to sputtering yields of the order of 100 [6]. As the spike size is typically of the order of a few nanometers, it is interesting to pose the question of whether ion-irradiation of nanostructures may give rise to enhanced sputtering due to the possibility of a single atomic cascade and thermal spike intersecting with, not only the top surface (on which the ion impacts), but also the side and bottom surfaces of the structure. Previous MD simulations have reported a sputtering enhancement resulting from cascade interaction with the surface [7], and experiments have shown that sputtering yields of secondary molecular ions can be dramatically enhanced by the presence of metal nanoclusters on the surface of an organic material [8]. However, to our knowledge, there are no previous experimental results on the sputtering yield of individual single nanostructures.

In this Article we report on *in-situ* Transmission Electron Microscopy (TEM) experiments of the changes occurring in Au nanorods under irradiation, at room temperature, by 80 keV Xe ions and on MD simulations of the same irradiation conditions and nanostructure size as in the experiments. Sputtering yields, $S$, have been calculated that are greater than those measured for a flat surface by more than an order of magnitude. Recent work indicates an expected increased in sputtering yield from ballistic ejection and evaporative loss of

approximately a factor of four when comparing nanorods with flat surfaces; other factors, however, must be taken into consideration in order to explain the dramatically enhanced yields observed [9]. In the current paper we present the experimental results and further details on the MD simulation results with a focus on "explosive" ejection of nanoclusters and the varied angles of incidence that pertain to ion irradiation of nanorods.

## 2. Experiments

Au nanowires were irradiated with 80 keV $Xe^+$ ions at room temperature in a JEOL JEM-2000FX TEM operating at 200 keV in the MIAMI facility at the University of Huddersfield [10]. The ion flux was maintained at $2.1 \pm 0.2 \times 10^{11}$ ions $cm^{-2}$ $s^{-1}$ and the fluence range over which volume measurements were made was $0.0 - 2.6 \times 10^{14}$ ions $cm^{-2}$. The ion beam was incident on the specimen at 30º to the direction of the electron beam, giving an ion range of approximately 11 nm, calculated by the Monte Carlo computer code SRIM [11]. A Gatan Orius camera was used to record images of resolution 480 × 480 pixels, as a video sequence of 8 fps.

The original Au nanowires were produced by electrodeposition of gold into an anodic aluminum oxide template that has pores of 20 nm diameter. The template was then dissolved in a bath of 0.1 M NaOH leaving gold nanowires. These were subsequently deposited onto holey-Formvar-coated Cu TEM grids where they were generally flat on the Formvar film. Electron microscopy indicated that the nanowires were approximately 20 nm in diameter, microns in length and consisted of columnar grains along the wire. Electron diffraction analysis revealed no texturing (or preferred growth direction) of the grains that were generally 100 nm in length.

Under irradiation the nanowires were observed to "neck" and subsequently separate at grain boundaries. FIG. 1a shows a nanowire that has fragmented into nanorods after irradiation to a fluence of $1.9 \times 10^{14}$ ions $cm^{-2}$. Small Au particles are clearly visible around the nanorods that are from sputter-deposition of Au onto the Formvar film.

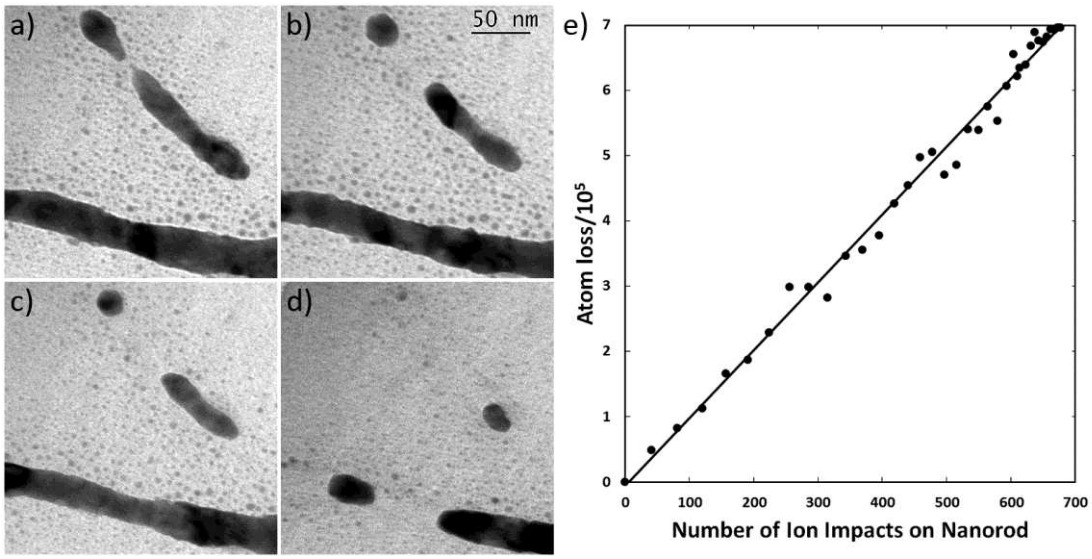


FIG 1. Observations of Au nanowires under irradiation with 80 keV Xe ions. Bright field TEM images: a) formation of nanorods due to separation at grain boundaries, following irradiation to a fluence of 1.9 x $10^{14}$ ions $cm^{-2}$; b) nanorod at the starting point for volume measurements; c) nanorod following irradiation with an additional fluence of $6.0 \times 10^{13}$ ions $cm^{-2}$ (≈ 342 impacts on nanorod) d) nanorod following irradiation with an additional fluence of $2.2 \times 10^{14}$ ions $cm^{-2}$ (≈ 342 further impacts on nanorod). e) Plot of atom loss versus ion impacts for Au nanorod shown in panels b) to d).

At all stages of the irradiation, diffraction contrast is observable in the nanorods indicating that, as in the case of ion irradiation of Au foils, the Au nanorods retain their crystallinity throughout the irradiation. The changes to the shape and size of the rod result from a combination of loss of atoms by sputtering and redistribution of atoms by localized flow processes [1–4].

To confirm that the nanorods maintained their cylindrical symmetry during the irradiations, a series of tilts were performed in two experiments, ±50º in 10º steps about the axis of the individual nanorods, with the nanorods ultimately becoming spherical nanoparticles.

To determine $S$, video stills were taken at intervals of 30 seconds ($6.3 \times 10^{12}$ ions/cm$^2$) with an example shown in FIG. 1b. From these images a volume, $V$, of the nanorod was determined by measuring the radius, $r_i$, along the axis of the nanorod at intervals, $\Delta x_i$, of 0.46 nm (2 pixels). The volume is thus the sum:

$$V = \sum_i r_i^2 \, x_i \qquad \text{..... (1)}$$

The number of atoms in the nanorod at any time step is then calculated as the volume multiplied by the atomic density of gold (58.98 atoms/nm$^3$). The number of ions that impact on the nanorod was determined from the fluence and the projected area of the nanorod, with a trigonometric correction for the angle between electron and ion beams. FIGs. 1 c) and d) show the evolution of Au nanorods under heavy-ion irradiation. FIG. 1e shows the data for a nanorod where $S$ was found to be 1036±87 atoms/ion. Additional experiments have been performed for which $S$ was calculated to be 1887±207, 823±85, 175±21 and 147±12 atoms/ion. In three experiments, $S$ is much greater than the value obtained for 80 keV Xe ions on Au surfaces of approximately 50 [6] although it should be noted that this figure could be at least 3 or times higher for some non-normal angles of incidence [12]. For the nanorod with a measured sputtering yield of 147, diffraction analysis showed that the ion beam was aligned with a <112> direction (±2°). Further investigation has shown that channeling can have a large effect in irradiations of Au nanostructures [9].

## 3. Simulations and discussion

We have previously concluded that ballistic sputtering or sputtering considered as a classical evaporation process cannot explain the observed sputtering yields [9]. In the current paper, we present details of our MD simulation results on the sputtering and focus on the angular dependence of $S$ and on the emission of clusters. The former is of obvious relevance given that a wide range of incidence angles are inevitably present when ion irradiating a cylinder (or and hemispherical end caps). The increased importance of the emission of clusters of atoms when ion irradiating nanostructures is an important finding of this work.

MD simulations were performed in order to investigate the sputtering processes on the atomic level and better understand the reasons for the high yields. An Au nanowire with dimensions typical of those used in the experimental work (70 nm in length and 20 nm in diameter with hemispherical ends), was irradiated sequentially by individual 80 keV Xe ions. Interactions between Au atoms were modelled with the Foiles et al. [13] embedded-atom method (EAM) potential. This fairly well represents various Au properties crucial for sputtering simulations suc as the surface energy and the melting temperature [14]. It has also demonstrated a good agreement with experimental results in the simulation of surface irradiation effects [3,15,16,17] which is important for a realistic modelling of high energy Xe ions impacts on Au nanowires. To simulate high-energy collisions in cascades produced by Xe ions impacts the universal Ziegler–Biersack–Littmark (ZBL) repulsive potential [18] was applied at small interatomic distances to complement the EAM potential. The ZBL electronic stopping model was applied for all atoms which had a kinetic energy ≥ 5 eV [19,20]. More details of MD simulations of ion impacts on Au samples have been given elsewhere [21,22].

Xe ions were fired from random sites above the nanowire with the angles between the nanowire axis and the ion trajectories selected randomly in the range 90° ± 20°. The nanowire's upper plane represented a (100) Au surface. We have estimated that the nanowire's maximal temperature after each impact cannot exceed 800 K when irradiated by 80 keV Xe ions. Using the black body radiation law, we conclused that radiative cooling of the nanowire can be neglected in this case. After each irradiation the system was relaxed for 200 ps without any temperature control algorithms. All sputtered atoms and clusters were then removed and the nanowire was cooled down to 300 K. This should imitate the experimental situation of a thermal conductive cooling through the Formvar film.

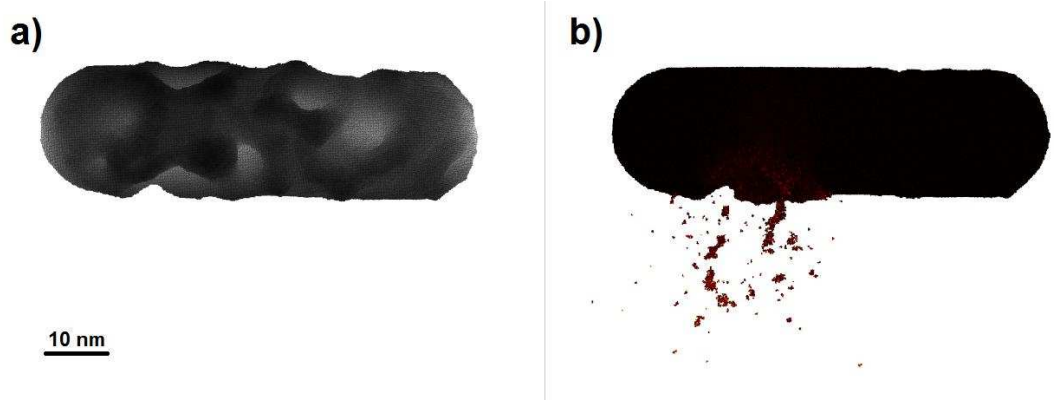


FIG. 2: Results of MD irradiation simulations of 80 keV Xe ions impacts on an Au nanowire: a) Final shape of the nanowire after 32 ion impacts; lighter color represents deeper atomic layers b) Snapshot at 25 ps following a single ion impact showing a formed crater and ejected nanoclusters. Clusters smaller than three atoms in size and individual atoms were removed from the picture for a better visibility.

The final shape of the nanowire following 32 ion impacts is presented in FIG 2a. Deeper atomic layers are colored in gray to enhance the visibility of craters formed after the impacts. Although similar craters are observed for some ion impacts in our experiment, they generally disappear during subsequent impacts. This can be explained by ion-induced localized flow events coupled with surface tension effects[2] which happen when impact points are close to the previous ones and which results in a smoothing of the surface roughness. The number of impacts simulated by MD was much smaller than those occurring during an experiment and this may partially explain the greater number of individual craters observable in the MD simulations.

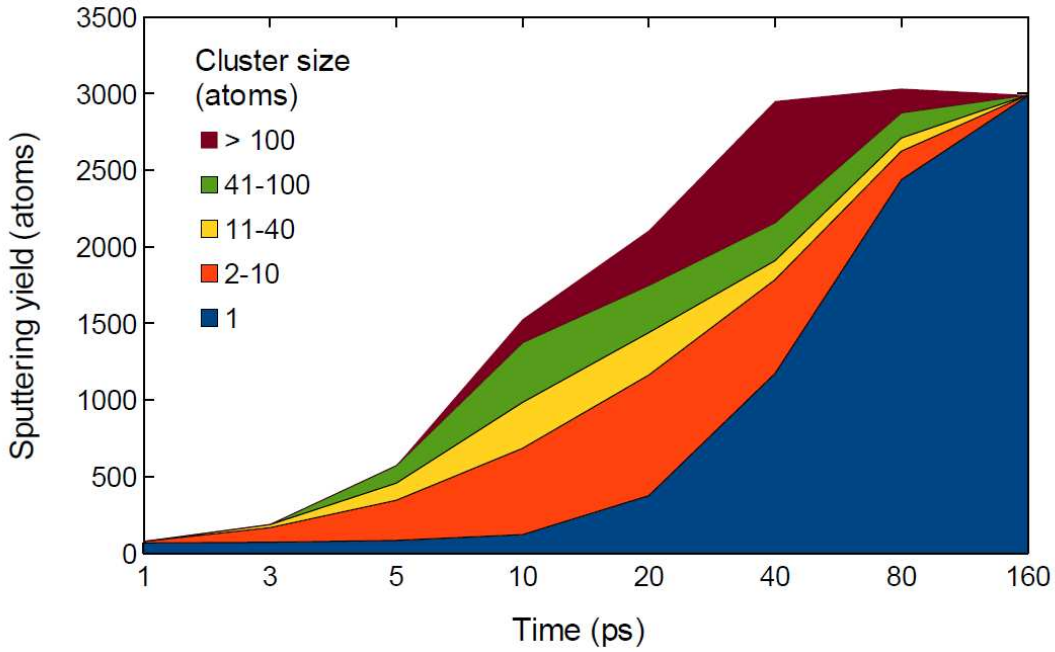


FIG. 3: Area chart showing a contribution of Au nanoclusters of different size to the total yield over time for the single 80 keV Xe ion impact shown in FIG. 2b. The predominance of the blue curve at 80–100 ps is due to the fact that all of the nanoclusters have disintegrated by the end of the simulation for this event. For other impacts the biggest clusters stay intact.

FIG 2b clearly shows the emission of clusters due to a single ion impact, an important component of the sputtering yield which is generally not taken into account in sputtering models. Clusters are ejected as a result of thermal spike events and appear to provide the major component of the giant yields. This can be seen in FIG 3, where the contribution of nanoclusters of different size to the total sputtering yield for the single event is presented. At 10 ps more than 90% of the ejected Au was in the form of clusters. The biggest clusters were mainly ejected during the latest stages of the spike event: from 20 to 40 ps. By the end of the simulation, however, the ejected atoms are entirely in the form of individual atoms as all of the clusters have evaporated. Note that we have not implemented a radiative cooling model; it was not necessary for the nanowire itself due to the assumption of conductive cooling via the Formvar; however, this may be important for ejected nanoclusters with high temperature and big surface to volume ratios. Nevertheless, after several irradiation events, the biggest clusters were observed to be intact even at the end of the simulations. These observations are qualitatively similar to those in Ref. [17], where it was also reported that the clear majority of sputtered clusters break up. Clusters bigger than 100 atoms in size were observed in about 60% of all the non-channeling irradiation events.

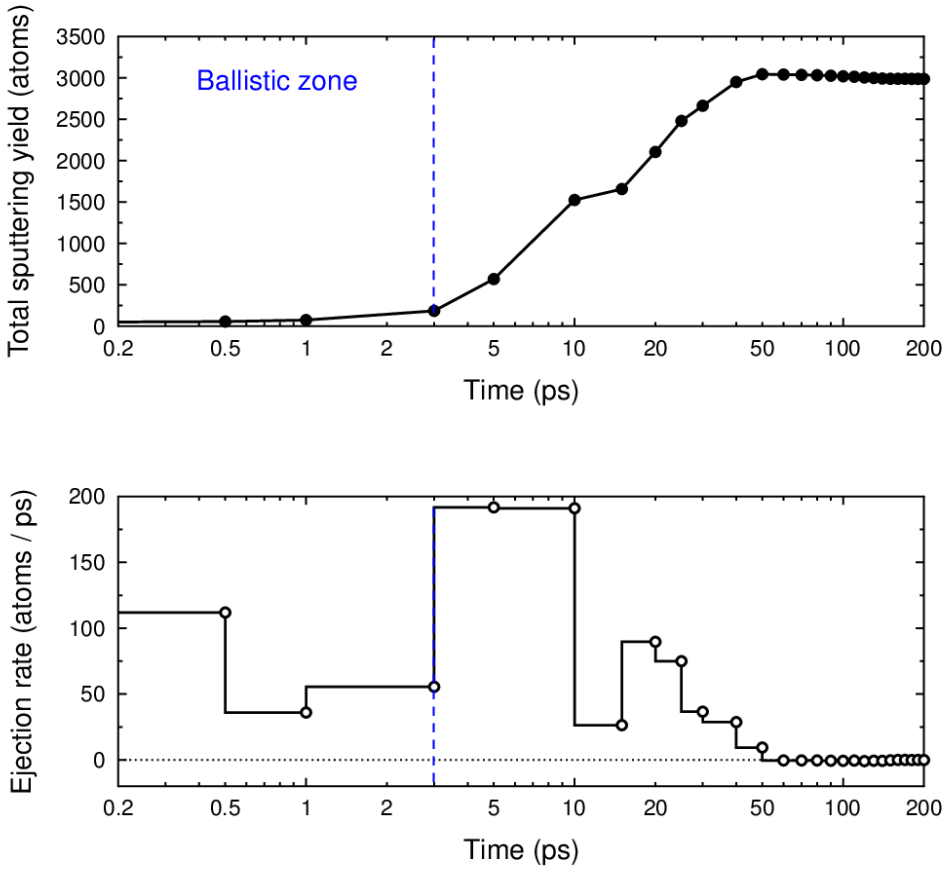


FIG. 4: Plot of a total sputtering yield and an ejection rate as a function of time for the single 80 keV Xe ion impact shown in FIG. 2b. Each point on the ejection rate plot represents the mean ejection rate for the period since the previous point. Ballistic and evaporative processes are expected to be responsible for the sputtering up to 3ps. The decrease of the total yield from 60 ps is due to redeposition processes (cf. Ref. [17]).

The ejection rate as a function of time for the event depicted in FIG. 2b, with a corresponding sputtering yield presented in FIG. 4. This graph clearly demonstrates that the main contribution to the total yield was given by clusters emitted as a result of the thermal spike process and takes place due to a localized melting and "explosive" ejection of the molten material. The total number of atoms ejected by ballistic and evaporative processes was about 150, while the total yield was 2980 for this event. After 60 ps, negative ejection values are observed, and the total number of sputtered Au atoms has decreased by about 30 atoms due to the redeposition effect: when hot sputtered clusters break up by evaporation, the atoms go in random directions, and some are redeposited on the nanorod [17]. The average yield from 32 simulated impacts was 980±180, with the maximal value for a single impact of 3159 sputtered atoms. When the incident Xe ion was aligned with the channelling direction the yield decreased to 0, because of the very small amount of energy transmitted from the ion to the nanowire when channeling occurs.

Range calculations were performed with the MDRANGE code [23] to assess the influence of channelling on sputtering yields. This method has already given a very good estimation of ion ranges in crystal channels in GaN and GaAs samples of different orientations [24,25]. Au monocrystalline samples with upper surface normals in the <100>, <110>, <111> and <112> crystal directions were prepared; Au atoms were displaced randomly from the equilibrium positions according to the Debye model with a Debye temperature of 170 K [26] which

should represent thermal displacements at 300 K. ZBL electronic stopping [18] was applied to the Xe ions. The twist angle φof the incident ion was selected randomly. The calculated half-angle for channeling for 80 keV Xe ions on Au was from 3° to 5° for these four directions, which is in a good agreement with the experimental results [25]. The calculated ranges were 4–10 times longer than the mean value of 12.2±0.2 nm for the non-channeling directions. As the diameter of the nanowire was 20 nm, channeling thus results in only a small amount of energy transferred from channeled Xe ions to the nanowire.

It is known that sputtering yields can be enhanced by off-normal incoming angles [27,28], and the irradiation of a nanowire will involve all possible incoming angles with respect to the surface normal. Hence we also simulated the sputtering yield of a flat Au surface at incoming angles between 0 and 85 degrees off-normal. The results are shown in Fig. 5.

Using a CAD model of the nanorod (cylinder with hemispherical caps) and with the appropriate geometry we numerically determined the distribution of ions over the various angles of incidence. Combining this with the data in Fig. 5 then enabled us to estimate the sputtering yield due to the effects of the varied angles of incidence that are present for ion irradiation of the nanorod. This gives an enhanced value of S = 389, much more than the flat surface yield but still less than the nanowire yields of ~1000. This shows that the enhanced sputtering yield can only partly be attributed to off-normal incidence angles at the nanowire.

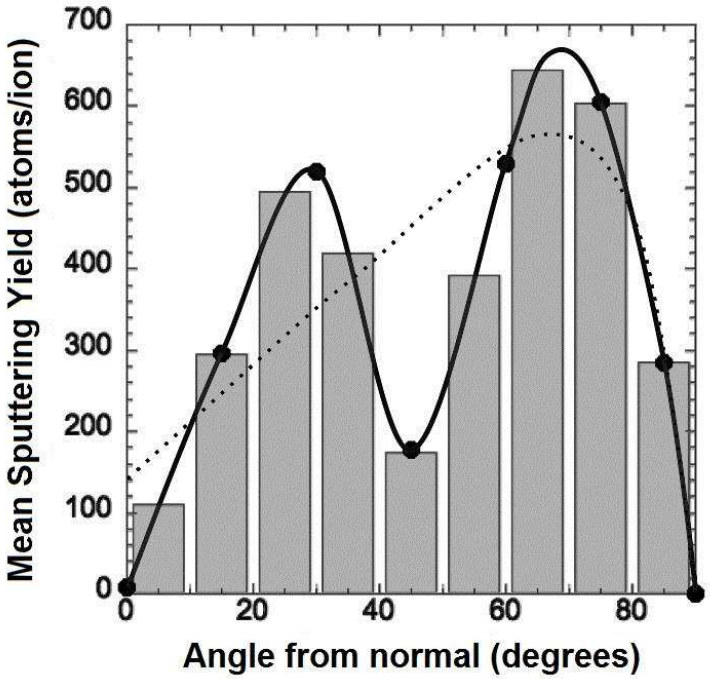


FIG. 5. MD simulation results of the angular dependence of the sputtering yield of a flat Au (100) surface. Note that the sputtering yield vs. angle curve has a low value at 0 and 45 degrees due to channeling. For a different orientation with respect to the Au lattice, which avoided channeling, the yield at these angles would be higher but the peaks in the curve would also be lower. The solid line is a polynomial fit to the data. The dotted line is a sketch of what this might look like if the orientation wrt to the crystalline structure were chosen to avoid aligning with channels. I.e. on either side of the channeling dips (in angular terms), the ions experience a "higher than random" density.

In order to check whether the cluster emission is specific to the nanorod geometry, or whether it can also be observed during the irradiation of flat Au surfaces, we analyzed the size of the largest sputtered clusters in both cases. We found that the average size for the biggest

sputtered cluster from the nanowire simulations was 400 atoms, wheres for the bulk cases it was 200 or less for all incoming angles. The number of clusters emitted in the nanorod irradiations was also greater.

The larger surface area and surface curvature of a nanorod gives rise to the emission of a significantly larger number of atoms in clusters than in the case of ion irradiation of a flat surface.

## 4. Conclusions

Using both experiments and simulations we have shown that the sputtering yield from single Au nanorods, with diameters of about 20 nm, can exceed 1000. This major enhancement of the sputtering yield compared to flat surfaces is due to enhanced sputtering at off-normal incidence angles and "explosive" emission of atomic clusters due to the thermal spikes, which is enhanced in the nanorod due to the proximity of surfaces.

**Acknowledgements.**

The sponsorship of the Academy of Finland through the research project COMOMEN (#1139204) is thankfully acknowledged. We are very grateful for the computational resources granted by the Center for Scientific Computing in Espoo, Finland

[1] R. C. Birtcher, S. E. Donnelly, Phys. Rev. Lett. **77** (21) 4374 (1996).
[2] S. E. Donnelly, R. C. Birtcher Phys. Rev. B **56** (21) 13599 (1997).
[3] K. Nordlund , J. Tarus, J. Keinonen , S. E. Donnelly, R.C. Birtcher, Nucl. Instrum. Meth. B **206** 189 (2001).
[4] S. E. Donnelly, R. C. Birtcher, Philos. Mag. A **79**(1) 133-145 (1999).
[5] J. A. Brinkman, J. Appl. Phys. **25** (8) 961 (1954).
[6] H. H. Andersen, H. L. Bay, in *Sputtering by Particle Bombardment I* (Topics in Applied Physics **47**), R. Behrisch (Ed), 145, Springer Berlin Heidelberg (1981).
[7] T. T. Järvi, J. A. Pakarinen, A. Kuronen, K. Nordlund, Europhys. Lett. **82** 26002 (2008).
[8] A. Marcus, N Winograd, Anal. Chem. 78 (1) 145 (2006)
[9] G. Greaves, J. A. Hinks, P. Busby, N. J. Mellors, A. Ilinov, A. Kuronen, K. Nordlund, and S. E. Donnelly, Giant Sputtering Yields from Single-Ion Impacts on Gold Nanorods, Phys. Rev. Lett. (2013), accepted for publication.
[10] J. A. Hinks, J. A. van den Berg, S. E. Donnelly, J. Vac. Sci & Technol. A **29**(2) 021003 (2011)
[11]: J.F. Ziegler, M.D. Ziegler, J.P. Biersack, Nucl. Instr. and Meth. B 268 (2010) 1818-1823
[12] J. M. Fluit, P. K. Rol, and J. Kistemaker, J. Appl. Phys. **34**, 690 (1963).
[13] S. M. Foiles, M. I. Baskes, and M. S. Daw, Phys. Rev. B, 33(12) 7983 (1986). Erratum: ibid, Phys. Rev. B **37** 10378 (1988).
[14] M. S. Daw, S. M. Foiles, M. I. Baskes. Mat. Sci. Rep. **9** 251 (1993)
[15] J. Samela, J. Kotakoski, K. Nordlund, J. Keinonen, Nucl. Instr. and Meth. B **239** 331 (2005).
[16] M Ghaly, R. S. Averback. Phys. Rev. Lett., **72**(3) 364 (1994)
[17] K.O.E. Henriksson, K. Nordlund, J. Keinonen, Phys. Rev. B **71** 014117 (2005)
[18] J.F. Ziegler, J.P. Biersack, U. Littmark, The Stopping and Range of Ions Matter, Pergamon, New York, USA, (1985).
[19] K. O. E. Henriksson, K. Nordlund, and J. Keinonen. Nucl. Instr. Meth. B **255**(1) 259 (2007)
[20] K. Nordlund. Comput. Mater. Sci. **3** 448, (1995).
[21] J. Samela, K. Nordlund, Nucl. Instrum. Meth. **B** 263 375 (2007)
[22] K. Nordlund, M. Ghaly, R. S. Averback, M. Caturla, T. Diaz de la Rubia, J. Tarus, Phys. Rev. B, **57**(13) 7556 (1998).
[23] J. Sillanpää, K. Nordlund, J. Keinonen, Phys. Rev. B, **62** 3109 (2000).
[24] J. Peltola, K. Nordlund, J. Keinonen. Nucl. Instr. Meth. B, **212** 118 (2003).
[25] J. Nord, K. Nordlund, B. Pipeleers, and A. Vantomme. Mater. Sci. & Eng. B,**105**(1) 110 (2003).
[26] 27 N. W. Ashcroft and N. D. Mermin, *Solid State Physics*, (Saunders College, Philadelphia,1976).

[27]: G. Wehner, J. Appl. Phys. **30** 1762 (1959).
[28]: J. M. Fluit, P. K. Roi and J. Kistemaker, J. Appl. Phys. 34 690 (1963).